Carbon-13 NMR Relaxation Studies of Cycloalkylidene Bisphenols, Methyl Ethers, and Simple Benzoate Esters in Solution: Different Average Correlation Times for Dipole–Dipole and Chemical Shift Anisotropy Relaxation

Young-Hwa Lee, Bruce D. Allison,[†] and John B. Grutzner*

Department of Chemistry, Purdue University, West Lafayette, Indiana 47907-1393

Received: September 2, 1993; In Final Form: November 23, 1993[●]

Carbon-13 NMR relaxation of a series of cycloalkylidene bisphenol monomers and related compounds has been examined. The following monomers were studied: cyclohexylidene bisphenol and its dimethyl ether, 4-*tert*-butylcyclohexylidene bisphenol and its dimethyl ether, cyclopentylidene bisphenol, phenyl 1,3,5-tribenzoate, and triphenyl 1,3,5-benzenecarboxylate. The motional properties of these compounds in solution have been determined from their carbon T_1 relaxation times. Phenyl motion is generally faster than overall molecular tumbling except for the axial group of tBBP6. The order of phenyl mobilities was TPBC > PTB > tBBP6 eq ~ BP5 > BP6 > tBBP6 ax. In PTB and TPBC dipole–dipole (DD) coupling relaxes the protonated carbons, and chemical shift anisotropy (CSA) is a major contributor for substituted carbons, especially at 150 MHz. Different average diffusional correlation times were found for DD and CSA relaxation for the fast internal phenyl motion. Small-angle rotational diffusion about the phenyl C_2 axis was inferred to be faster than overall tumbling, but complete rotational averaging was slower. Three bond ^{13}C–H coupling constants were measured for PTB and TPBC. The ^{13}C isotope-induced shift for H2 of PTB was 2.0 ppb. The activation energy for ring inversion in BP6 was measured to be 11 ± 1 kcal/mol.

Internal molecular motion of bisphenol units in polymers plays an important role in their dynamic mechanical properties.[1-10] For example, modifying either the alkyl unit[1-4] or the aromatic unit[1,2,4,5] can change glass transition temperatures and mechanical loss peaks by over 50 K. Sundarajan[3] has shown that replacing the isopropylidene group with the more rigid cyclohexylidene group significantly inhibits the phenyl motion. Morbitzer and co-workers[1] and McHattie et al.[2] have shown that the bulk physical properties of impact resistance and gas permeability can be modified by changing the alkylidene unit. As part of our systematic study of the influence of alkyl group mobility on dynamic properties, we have studied a series of cycloalkylidene bisphenol monomers, ethers, and polycarbonates.[11] In this paper we report the ^{13}C NMR spectra and carbon T_1 relaxation times of the monomeric systems cyclopentylidene bisphenol, BP5; cyclohexylidene bisphenol, BP6; and 4-*tert*-butylcyclohexylidene bisphenol, tBBP6, and their methyl ethers, BP6M and tBBP6M. The 4-*tert*-butyl substituent prevents ring inversion of the cyclohexane ring, and the axial and equatorial phenyl groups are distinguished. The symmetrical esters, triphenyl 1,3,5-benzenetricarboxylate (TPBC) and phenyl 1,3,5-tribenzoate (PTB), were included to provide information about phenyl ester dynamics.

Carbon-13 T_1 Relaxation and Molecular Dynamics.[12-15] Carbon-13 NMR T_1 relaxation times are sensitive indicators of molecular motion in solution on the time scale of microseconds to picoseconds. They have been used to study dynamics in a wide range of systems from small molecules to large polymers. For protonated carbons, ^{13}C relaxation times, T_1, are dominated by the nuclear dipole–dipole interaction with the attached protons. T_1 of a ^{13}C nucleus in a $^{13}CH_n$ group relaxed by interaction with the attached protons is given by

$$\frac{1}{T_1^{\mathrm{DD}}} = \frac{1}{20}\left\{\frac{\mu_0}{4\pi}\right\}^2 \frac{n\gamma_H^{\,2}\gamma_C^{\,2}\hbar^2}{r_{\mathrm{CH}}^{\,6}}\{J(\omega_H - \omega_C) + 3J(\omega_C) + 6J(\omega_H + \omega_C)\} \quad (1)$$

where μ_0 is the permeability constant, $\hbar$ is the Planck constant divided by 2π, γ_H and γ_C are the magnetogyric ratios for ^1H and ^{13}C, respectively, r_{CH} is the C–H internuclear distance, ω_H and ω_C are the ^1H and ^{13}C resonance frequencies, respectively, and $J(\omega)$ is the spectral density function. When a molecule reorients by isotropic rotational diffusion with diffusion constant D, the

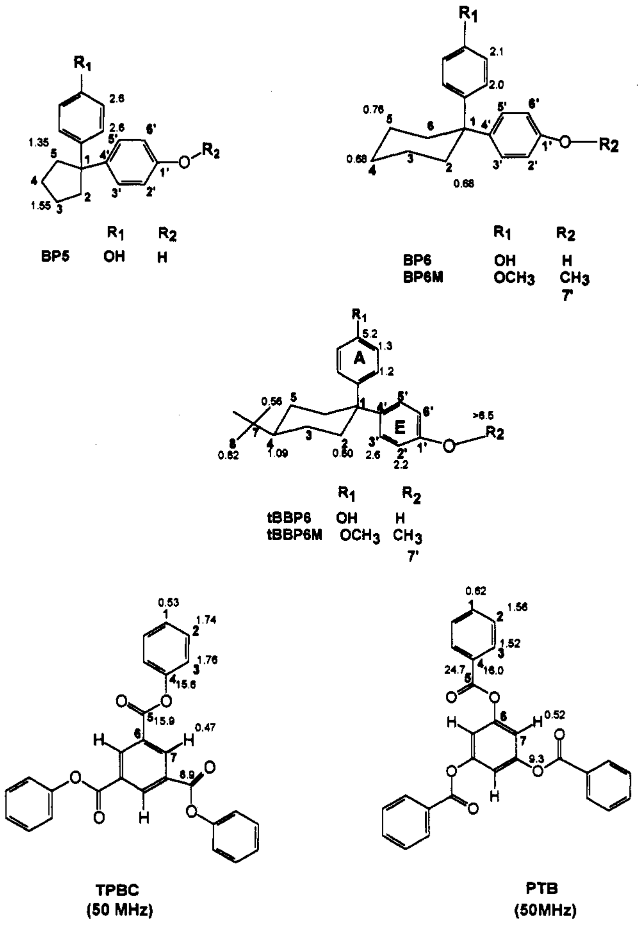

Structures and Carbon-13 (100 MHz) Relaxation Times (s).

[†] Permanent address: Department of Chemistry, Ross-Hulman Institute of Technology, Terre Haute, IN 47803.

[●] Abstract published in *Advance ACS Abstracts,* January 15, 1994.

0022-3654/94/2098-1783$04.50/0

spectral density is given by

$$J(\omega) = 2\tau_c/(1 + \omega^2\tau_c^2) \tag{2}$$

where τ_c is the rotational correlation time for each C–H dipole, which is equal to $(6D)^{-1}$. When a small organic molecule undergoes rapid reorientation in solution, the extreme narrowing condition, $\omega^2\tau_c^2 \ll 1$ is usually satisfied. Under this limit, eq 1 simplifies to

$$\frac{1}{nT_1^{\mathrm{DD}}} = \left\{\frac{\mu_0}{4\pi}\right\}^2 \frac{\gamma_H^2\gamma_C^2\hbar^2}{r_{CH}^6}\tau_c \tag{3}$$

For an isotropically reorienting molecule, the rotational correlation time is related to the solution viscosity and the radius of the molecule by

$$\tau_c = \frac{Vf_{GW}\eta}{kT} = \frac{4\pi r_0^3 f_{GW}\eta}{3kT} \tag{4}$$

where η is the solution viscosity and r_0 and V are the mean radius and the volume of the solute molecule, respectively. f_{GW} is the Gierer–Wirtz[16] empirical factor which depends on the ratio of solvent to solute radii, r_s/r_0

$$f_{GW}^{-1} = 6\left[\frac{r_s}{r_0}\right] + \left[1 + \left(\frac{r_s}{r_0}\right)\right]^{-3} \tag{5}$$

A detailed review of molecular rotation and anisotropic T_1 relaxation has been published.[13]

The anisotropy of the chemical shielding tensor may also provide the oscillating magnetic field required for spin–lattice relaxation. Under the conditions of an axially symmetric shielding tensor and extreme narrowing, the CSA contribution to the spin–lattice relaxation is given by

$$\frac{1}{T_1^{\mathrm{CSA}}} = \frac{2}{15}\gamma_C^2 B_0^2(\sigma_\parallel - \sigma_\perp)^2\tau_c \tag{6}$$

where B_0 is the applied magnetic field and $\sigma_\parallel$ and $\sigma_\perp$ are the parallel and perpendicular components of the shielding tensor, respectively. The CSA mechanism plays a significant role for quaternary aromatic carbon relaxation, especially at high magnetic field.[12]

When more than one mechanism is involved in the relaxation of a particular nucleus and cross-relaxation between mechanisms is ignored, the observed T_1 is assumed to be given by the sum of the relaxation rate from the individual mechanisms.[13]

$$\frac{1}{T_1} = \sum_i \frac{1}{T_1^i} \tag{7}$$

where summation is over the i different mechanisms. The neglect of cross-relaxation contributions from DD and CSA mechanisms under decoupled conditions has been validated by Farrar for systems with a single correlation time.[17]

The contribution of each individual mechanism to the measured T_1 can be evaluated from the characteristics of that mechanism. Only the dipole–dipole mechanism gives rise to double- and zero-quantum transitions, W_2 and W_0, respectively. For dipolar relaxation of a ^{13}C–H spin system, the ^{13}C nuclear Overhauser effect (NOE) is observed when the protons are decoupled.

$$\mathrm{NOE} = \frac{S^d}{S^0} = 1 + \frac{\gamma_H}{\gamma_C}\left(\frac{6J(\omega_H + \omega_C) - J(\omega_H - \omega_C)}{6J(\omega_H + \omega_C) + 3J(\omega_C) + J(\omega_H - \omega_C)}\right) \tag{8}$$

where S^d and S^0 are the ^{13}C integrated intensities with and without proton decoupling, respectively. The limits of the NOE are 2.988 for $\omega^2\tau_c^2 \ll 1$ and 1.154 for $\omega^2\tau_c^2 \gg 1$ where ω is the largest frequency in the spectral density, i.e., $\omega = \omega_H + \omega_C$. When $\tau_c = 1.0 \times 10^{-10}$ s and $\omega_C = 150$ MHz (i.e., $\omega^2\tau_c^2 = 0.22$), the NOE is estimated to be 2.799 by eq 8. When molecular motion satisfies the extreme narrowing limit, and the NOE deviates from its maximum value, other mechanisms besides dipole–dipole contribute to the observed T_1. Quantitative NOE measurements were only done for the polycarbonates derived from the bisphenol monomers.[11] Values greater than 2 were observed for all protonated carbons, confirming dipole–dipole relaxation. For the monomers reported here qualitative observations of relative peak intensities showed essentially maximum NOE's for all protonated carbons (Figure 1).

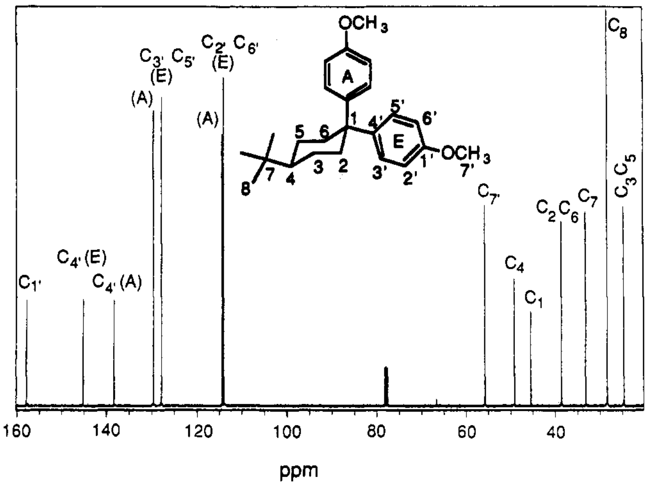

Figure 1. Proton-decoupled ^{13}C NMR spectrum of tBBP6M in CDCl$_3$ at 100.6 MHz.

Contributions from chemical shift anisotropy can be isolated by determining the applied field (B_0) dependence of the measured T_1. The maximum contribution of the CSA mechanism to the observed T_1 relaxation of the protonated ^{13}C nuclei in this work is estimated by substitution in eqs 3 and 6 as 15% when $\omega_C^2\tau_c^2 = 10^{-2}$ and $(\sigma_\parallel - \sigma_\perp) = 200$ ppm.

In a monosubstituted benzene, the T_1 for the para carbon is shorter than the T_1 for the ortho or meta carbons of the same phenyl ring.[18] This occurs because rotational diffusion is most rapid around the C_2 phenyl symmetry axis, which is coincident with the C–X bond. The simplest model of anisotropic motion has been developed by Woessner[19] for axially symmetric molecules based on the reorientation of a rigid ellipsoid. In this model, the correlation times are expressed by two parameters, D_1 and D_2, which are the rotational diffusion constants about the major axis (C_2 axis) and the two perpendicular axes (minor axes), respectively.

$$\tau_c = \frac{1}{D_2}\left(\frac{A}{6} + \frac{B}{5 + \sigma} + \frac{C}{2 + 4\sigma}\right) \tag{9}$$

where $\sigma = D_1/D_2$ and the geometrical constants A, B, and C are given by the functions of the direction cosines of the angle between the direction of the magnetic interaction and the major rotation axis of the molecule.

$$\begin{aligned} A &= {}^1/_4(3\cos^2\theta - 1)^2 \\ B &= 3\cos^2\theta(1 - \cos^2\theta) \\ C &= {}^3/_4(1 - \cos^2\theta)^2 \end{aligned} \tag{10}$$

For a monosubstituted benzene, θ takes the values 60° and 120° relative to the C_2 axis for the ortho and meta carbon–hydrogen dipoles. In this case, the ratio of the correlation times

TABLE 1: ^{13}C Chemical Shifts, Relaxation Times T_1 (^{13}C), and Estimated Correlation Times, τ_c, for Substituted Bisphenols and Their Methyl Ethers

	BP5[a]		
	δ (ppm)	T_1 (s)[b]	$\tau_c \times 10^{11}$ (s)
C_3C_4	13.4	3.1 ± 0.1	1.8
C_2C_5	39.4	2.7 ± 0.1	2.0
C_1	55.0		
$C_{2'}C_{6'}$	115.4	2.6 ± 0.1	1.8
$C_{3'}C_{5'}$	128.5	2.6 ± 0.1	1.8
$C_{4'}$	140.9		
$C_{1'}$	155.8		

	BP6[c]			BP6M[d]		
	δ (ppm)	T_1 (s)[b]	$\tau_c \times 10^{11}$ (s)	δ (ppm)	T_1 (s)	$\tau_c \times 10^{11}$ (s)
C_3C_5	23.5	1.5 ± 0.1	3.7	22.7	1.2 ± 0.1	4.6
C_4	27.0	1.4 ± 0.1	3.9	26.2	1.1 ± 0.1	5.0
C_2C_6	37.9	1.4 ± 0.1	3.9	37.2	1.2 ± 0.1	4.6
$C_{2'}C_{6'}$	115.8	2.1 ± 0.1	2.2	113.5	1.7 ± 0.1	2.7
$C_{3'}C_{5'}$	129.0	2.0 ± 0.1	2.3	128.1	1.7 ± 0.1	2.7
C_1	45.4			44.9		
C_7				55.0	2.4 ± 0.1[e]	
$C_{4'}$	141.0			141.2		
$C_{1'}$	155.9			157.3		

	tBBP6			tBBP6M		
	δ (ppm)	T_1 (s)[b]	$\tau_c \times 10^{11}$ (s)	δ (ppm)	T_1 (s)[b]	$\tau_c \times 10^{11}$ (s)
C_3C_5	24.5	1.1 ± 0.1	5.0	23.6	0.70 ± 0.02	7.8
C_8	27.8	2.5 ± 0.1[e]		27.3	1.5 ± 0.1[e]	
C_2C_6	38.3	1.2 ± 0.1	4.6	37.6	0.60 ± 0.03	9.1
C_4	49.1	1.1 ± 0.1	5.0	48.2	0.63 ± 0.02	8.7
$C_{2'}C_{6'}$(E)	115.4	2.2 ± 0.1	2.1	113.3	1.5 ± 0.1	3.1
(A)	115.9	1.3 ± 0.1	3.6	113.7	0.74 ± 0.01	6.3
$C_{3'}C_{5'}$(E)	127.8	2.6 ± 0.1	1.8	127.2	1.4 ± 0.1	3.3
(A)	129.7	1.2 ± 0.1	3.9	129.1	0.71 ± 0.01	6.6
C_7	32.8			32.2		
C_1	45.1			45.5		
$C_{7'}$				55.0	1.7 ± 0.1[e]	
$C_{4'}$(A)	137.2	(5.2)[f]		137.8	(3.6)[f]	
(E)	144.2	(>6.5)[f]		144.7	(5.2)[f]	
$C_{1'}$	155.6			157.3		

[a] In acetone-d_6 at 50.3 MHz. [b] Values for protonated carbons are $nT_{1,\mathrm{obs}}$ where n is the number of directly bonded protons. [c] In acetone-d_6 at 100.6 MHz. [d] In CDCl$_3$ at 100.6 MHz. [e] Spin–rotation as well as dipole–dipole mechanisms may be involved in the methyl group relaxation. [f] Relaxation times for the quaternary carbons are approximate because the recovery delay was shorter than $5T_1$.

TABLE 2: ^{13}C Chemical Shifts, Coupling Constants, and Multiplicity, Relaxation Times T_1(^{13}C) Measured at 50.3 MHz in CDCl$_3$ and the Estimated Correlation Time τ_c

	δ (ppm)[a]	J (Hz)[b]	T_1 (s)	$\tau_c \times 10^{11}$ (s)
		TPBC		
C_1	126.9	$^1J = 162$, $^3J = 7$ (d, t)	0.53 ± 0.03	8.8
C_2	130.2	$^1J = 163$, $^3J = 8$ (d, d)	1.74 ± 0.09	2.8
C_3	122.1	$^1J = 164$, $^3J = 8$, $^3J' = 4$ (d, d, d)	1.76 ± 0.09	2.6
C_4	151.2	(m)	15.6 ± 0.8	
C_5	164.0	(m)	15.9 ± 1.0	
C_6	131.8	(s)	8.9 ± 0.8	
C_7	136.6	$^1J = 169$, $^3J = 6$ (d, t)	0.47 ± 0.02	9.9
		PTB		
C_1	134.4	$^1J = 161$, $^3J = 7$ (d, t)	0.62 ± 0.03	7.5
C_2	129.2	$^1J = 163$, $^3J = 8$ (d, d)	1.56 ± 0.08	3.0
C_3	130.8	$^1J = 163$, $^3J = 7$ (d, t)	1.52 ± 0.08	3.1
C_4	129.6	$^3J = 8$ (t)	16.0 ± 1.0	
C_5	165.1	(m)	24.7 ± 1.6	
C_6	152.8	(m)	9.3 ± 0.5	
C_7	113.8	$^1J = 168$, $^3J = 5$ (d, t)	0.52 ± 0.03	9.0

[a] Chemical shifts were referenced to internal TMS. [b] The apparent multiplicities are shown in parentheses. s = singlet, d = doublet, t = triplet, and m = multiplet.

for anisotropic motion to that in isotropic motion, τ_c/τ_0, is given by

$$\left(\frac{\tau_c}{\tau_0}\right)_{\mathrm{DD}} = \left(\frac{T_1(\mathrm{iso})}{T_1(\mathrm{aniso})}\right)_{\mathrm{DD}} = \frac{\sigma^2 + 262\sigma + 313}{64\sigma^2 + 352\sigma + 160} \qquad (11)$$

For an aromatic carbon in a rotating phenyl group relaxed by CSA, θ is 90°, and $\sigma_\parallel = \sigma_{11}$ and $\sigma_\perp = \sigma_{33}$.[20] This gives

$$\left(\frac{\tau_c}{\tau_0}\right)_{\mathrm{CSA}} = \left(\frac{T_1(\mathrm{iso})}{T_1(\mathrm{aniso})}\right)_{\mathrm{CSA}} = \frac{5 + \sigma}{2 + 4\sigma} \qquad (12)$$

Results

Spectral Assignment. The ^{13}C chemical shifts and T_1 relaxation times for the cycloalkylidene compounds are given in Table 1. Assignments were made based on multiplicities in off-resonance spectra, peak intensities, and substituent effects in related compounds. In 4-*tert*-butylcyclohexyl-substituted bisphenol, tBBP6, and its methyl ether, tBBP6M, axial and equatorial phenylene rings show different resonance frequencies (Figure 1). The resonance of the ipso carbon ($C_{4'}$) in the axial position is observed at lower frequency (7 ppm) than that of the equatorial as observed for phenylcyclohexane where the axial ipso carbon was 4.7 ppm to lower frequency.[21] Different resonance frequencies for the ortho and meta carbons were also observed for the axial and equatorial phenylene rings. T_1(^{13}C) values were used to assign the different chemical shifts. The observed T_1($C_{4'}$) in the axial position is shorter than that for the equatorial. Therefore, each frequency with shorter T_1 for the ortho and meta carbons is assigned to the axial phenylene ring. In both compounds, the peaks for the axial phenylene ring were observed at higher frequencies, 1.9 ppm for ortho and 0.4 ppm for meta carbons, respectively. The average resonance frequency for each carbon is comparable to the corresponding chemical shift for BP6 and BP6M, where cyclohexane ring flipping averages the conformationally induced chemical shift differences (see below).

For assignments of the conjugated esters, the apparent multiplicity and coupling constants from the proton coupled spectrum were also used. ^{13}C chemical shifts, the apparent multiplicity, and approximate coupling constants from the proton-coupled spectra together with T_1 values are summarized in Table 2. To differentiate the resonance frequencies of the ipso carbons in the aromatic rings of the conjugated esters, the coupling pattern of the 152.1-ppm region of the proton-coupled ^{13}C spectrum of PTB was analyzed as an A_2BX system by spin simulation.[22,23] The observed asymmetry in the spectrum, shown in Figure 2, was simulated by including a long-range ^{13}C isotope effect on the proton chemical shifts. The analysis gave as $\Delta\delta$(A–B) as 2.0 ppb (0.4 Hz) with $J_{AB} = 2.12$, $J_{AX} = 4.92$, and $J_{BX} = 0.81$ Hz. The root-mean-square (rms) error for the 12 assigned lines was 0.16 Hz. The ^{13}C/^{12}C-induced proton isotope chemical shift differences of benzene were reported[24,25] as $^1\Delta = 2.44$, $^2\Delta = 1.34$, $^3\Delta = 0.51$, and $^4\Delta = 0.33$ ppb. These results confirm that the 152.1 ppm resonance comes from C_6. A similar but less complete analysis of the coupled spectrum of the resonance at 151.2 ppm in TPBC confirmed it as C_4.

Cyclohexane Inversion. The spectrum of BP6 was measured as a function of temperature to determine the rate of ring inversion. As the temperature was lowered (Figure 3), the aromatic resonances broadened, and by −80 °C, the ipso carbons had resolved into separate resonances at 136.4 and 143.8 ppm. The process was analyzed using the McConnell formalism for two-site exchange between equally populated sites.[26] The activation energy for the process was determined to be 11 ± 1 kcal/mol from the coalescence temperature, 215 ± 2 K. Line shape calculations and an Arrhenius plot gave estimates of $\Delta H^\ddagger = 11 \pm 2$ kcal/mol and $\Delta S^\ddagger = 5 \pm 5$ cal/(K mol). These values are

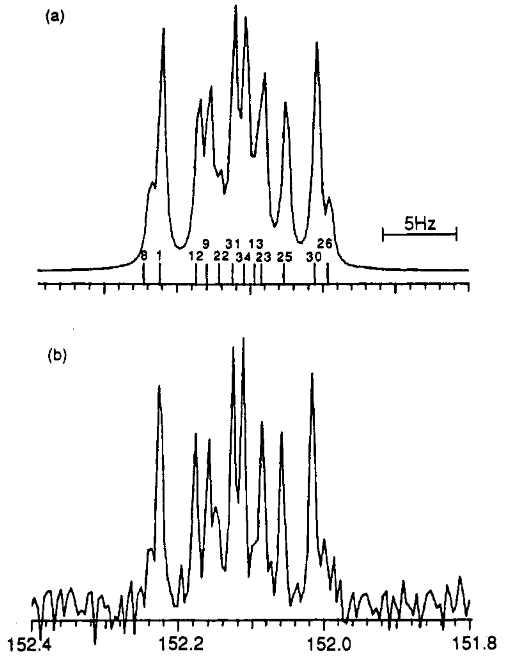

Figure 2. (a) Coupling pattern of the 152.1 ppm region of phenyl 1,3,5-tribenzoate. (b) Spin simulation spectrum with $\delta_A = 0.0$, $\delta_B = 0.4$, $\delta_X = 7654$, $J_{AB} = 2.12$, $J_{AX} = 4.92$, and $J_{BX} = 0.81$ Hz.

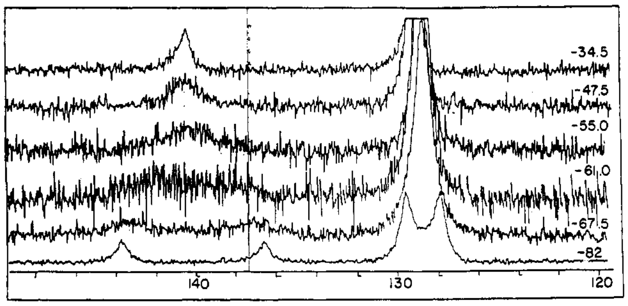

Figure 3. Aromatic region of 50-MHz ^{13}C NMR spectrum of BP6 as a function of temperature (°C): (a) -34.5, (b) -47.5, (c) -55, (d) -61.0, (e) -67.5, (f) -82.

similar to barriers determined for other 1,1-disubstituted cyclohexanes.[27] There is general agreement that the substituent pair has very little influence on the inversion barrier. The measured range is from 9.8 kcal/mol for 1,1-difluorocyclohexane to 11.4 kcal/mol for 1,1,4,4-tetramethylcyclohexane.

T_1 Relaxations and Their Field Dependence. Carbon T_1 relaxation times were measured by the inversion-recovery method and analyzed with a single-exponential curve fitting routine. T_1 values are estimated to be accurate to ±5%. The relaxation times for TPBC and PTB were determined as a function of magnetic field strength (Table 3 and Figure 4). The quaternary carbon relaxations show a linear dependence on B_0^2 showing that chemical shift anisotropy is the dominant relaxation field. The protonated carbon relaxation rates increased monotonically with field. The change is limited to about 10% between 50 and 150 MHz, consistent with predominant dipole–dipole relaxation for these protonated carbons.

The dipolar contribution to the observed relaxation times for the quaternary carbons is calculated from the intercept of the plot of $(T_1)^{-1}$ vs B_0^2 (Figure 4). To check the accuracy of this method, the dipolar contribution of the ortho protons to T_1's of C_6 in the esters was calculated using eq 3. The overall correlation time estimated from the $T_1(C_7)$ and $r_{CH} = 2.14$ Å for the ortho protons were used for this calculation. The calculated T_1^{DD} of C_6 (14 s, PTB; 13 s, TBPC) is the same as the dipolar contribution to T_1 observed from the intercept (13 and 12 s, respectively). To calculate T_1^{DD} of C_4, the correlation time estimated from T_1 (C_2, C_3) was used because internal phenyl rotation is the dominant motion for the dipolar relaxation of this nucleus. The C_4–H distances for this calculation were 2.14 Å for ortho protons, 3.38 Å for meta, and 3.85 Å for para. The calculated T_1^{DD} values were the same order of magnitude as the T_1^{DD} observed from the intercept of Figure 4 (40 s vs 20 s for PTB and 45 s vs 26 s for TPBC). Chemical shielding anisotropy dominated the observed relaxation rates for the quaternary carbons at 14.09 T with contributions of 73–90% (Table 4). The magnitude of the chemical shielding anisotropy may be estimated from the slope of the plot of $(T_1)^{-1}$ vs B_0^2 and the effective τ_c.

Discussion

The measured T_1 values and estimated correlation times for the protonated carbons of substituted bisphenols and their methyl ethers are summarized in Table 1, and those values for conjugated esters are given in Table 3. Correlation times for protonated carbons were estimated from the isotropic rotational tumbling model with eq 3. The C–H bond lengths used for estimation of the correlation times were 1.09 Å for aromatics and 1.12 Å for alicyclics. As $(\omega_C + \omega_H)^2\tau_c^2 \leq 0.02$, the extreme narrowing assumption is valid in these systems. For the small molecules studied, overall tumbling is the predominant motion responsible for relaxation, and similar nT_1 values are observed. For groups with low internal rotational barriers, however, additional fast motion reduced the efficiency of relaxation.

Based on molecular models, the cycloalkylidene bisphenols are propellor-shaped and approximately spherical. The shape of the esters depend on the bond angle at the ester oxygen. They could exist as flat discs or globular units with the three pendant rings on the same face of the central ring or as irregular oblate ellipsoids with the pendant rings on opposite faces.

Overall Tumbling. The uniformity of the correlation times for protonated carbons within each molecule shows that these compounds tumble like spheres in solution to a first approximation. Methyl and phenyl groups may have additional internal motion about their respective C_3 and C_2 symmetry axes. With the assumption of isotropic tumbling and eq 4, the size of the tumbling molecule may be estimated using the overall rotational correlation time. The viscosity of the solution was assumed to be the same as that of the solvent,[28] $\eta(CHCl_3) = 0.542$ cP and η(acetone) = 0.316 cP at 25 °C. The solvent radius was estimated as $r_s(CDCl_3) = 2.57$ Å and r_s(acetone-d_6) = 2.49 Å based on their van der Waals volumes.[29,30] The correlation times of the overall molecular tumbling estimated from the T_1's of the cycloalkyl rings and those of the central benzene rings in the conjugated esters were used to calculate the initial estimate of the molecular radius r_0 assuming $f_{GW} = 1$. This initial r_0 value and the solvent radius r_s were iterated to determine r_0 and f_{GW} with eqs 4 and 5. Converged values of r_0 and f_{GW} are summarized in Table 5.

The estimated r_0 values based on the overall molecular tumbling rate are comparable to the molecular radii measured from X-ray diffraction. The X-ray structures for the BP6, BP6M, tBBP6, and tBBP6M have been determined.[11,31] The X-ray distance from C_1 in the cyclohexyl ring to the phenolic hydrogen is 7.2 Å including the hydrogen van der Waals radius of 1.2 Å. In their methyl ethers, the distance from C_1 to the center of the methyl group is 7.7 Å. The diameter of the cyclohexyl ring from C_1 is about 5.1 Å, and the average distance from the *tert*-butyl group to C_1 is 7.2 Å. Therefore, the origin of the rotational motion is between C_1 of the cycloalkyl ring and the ipso carbons of the aromatic rings.

This shows that a single molecule is the unit of motion and that each ring within the molecule has the same effective length independent of dihedral angle. The estimated r_0 increases with increasing substitution among the bisphenols and their methyl ethers except for the BP6M. As shown in eq 4, the correlation time is directly proportional to the viscosity of the solution. The

TABLE 3: T_1 (s) of the Conjugated Esters at Various Magnetic Fields in $CDCl_3$[a]

	TPBC			PTB		
	7.05 T	11.74 T	14.09 T	7.05 T	11.74 T	14.09 T
C_4	9.8 ± 0.5	4.7 ± 0.3	3.5 ± 0.2	8.5 ± 0.4	4.9 ± 0.3	3.8 ± 0.2
C_5	10.1 ± 0.5	4.3 ± 0.3	3.5 ± 0.2	15.9 ± 0.8	6.9 ± 0.5	5.1 ± 0.3
C_6	6.9 ± 0.4	3.9 ± 0.2	3.0 ± 0.2	7.9 ± 0.4	4.9 ± 0.2	3.5 ± 0.2
C_1	0.58 ± 0.5	0.51 ± 0.03	0.50 ± 0.03	0.62 ± 0.03	0.59 ± 0.03	0.58 ± 0.03
C_2	1.72 ± 0.08	1.52 ± 0.08	1.45 ± 0.07	1.55 ± 0.08	1.42 ± 0.07	1.39 ± 0.07
C_3	1.79 ± 0.09	1.61 ± 0.08	1.52 ± 0.08	1.53 ± 0.08	1.43 ± 0.07	1.38 ± 0.07
C_7	0.54 ± 0.02	0.48 ± 0.02	0.48 ± 0.02	0.51 ± 0.03	0.53 ± 0.02	0.53 ± 0.02

[a] Data at 4.70 T were given in Table 2.

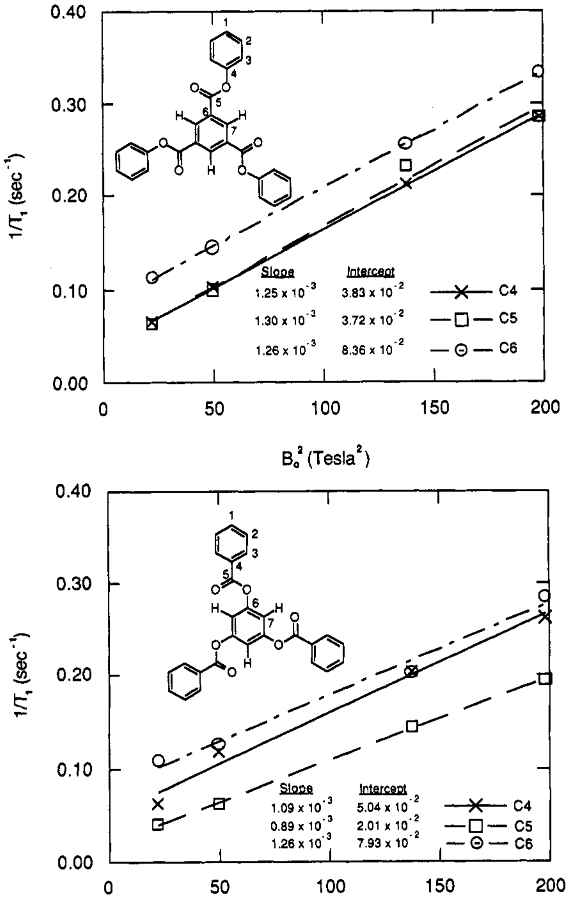

Figure 4. Plot of $(T_1)^{-1}$ vs $(B_0)^2$ of the quaternary carbons for (a, top) TPBC and (b, bottom) PTB in $CDCl_3$.

TABLE 4: Dipole–Dipole and Chemical Shift Anisotropy Contributions to T_1 and Estimated Magnitude of CSA for the Quaternary Carbons of the Conjugated Esters

	T_1^{DD} (s)[a]	$T_{1,cal}^{DD}$ (s)	T_1^{CSA} (s)[d]	$\tau_c \times 10^{11}$ (s)	$\Delta\sigma$ (ppm)[b]
			TPBC		
C_4	26 (13%)	45[c]	4.0 (87%)	2.7	288[d]
				9.9	145[e]
C_5	27 (13%)		4.0 (87%)	2.7	294[d]
				9.9	148[e]
C_6	12 (25%)	13[c]	4.0 (75%)	9.9	148
			PTB		
C_4	20 (19%)	40[c]	4.7 (81%)	3.1	254[d]
				9.0	142[e]
C_5	50 (10%)		5.7 (90%)	3.1	230[d]
				9.0	128[e]
C_6	13 (27%)	14[c]	4.8 (73%)	9.0	136

[a] T_1^{DD} estimated from the intercept of Figure 4 and T_1^{CSA} estimated from $(T_1^{CSA})^{-1} = (T_{1,obs})^{-1} - (T_1^{DD})^{-1}$. The percent contribution to the relaxation rate at 14.09 T is given in parentheses. [b] The CSA ($\Delta\sigma$, ppm) was determined from the slope of Figure 4 using eq 6 and τ_c as indicated. [c] Calculated dipolar contribution to T_1 assuming τ_c for overall tumbling motion from eq 3. [d] Estimated chemical shielding anisotropy assuming τ_c for internal rotation. [e] Estimated chemical shielding anisotropy assuming τ_c for overall tumbling motion.

TABLE 5: Average Correlation Times for Overall Tumbling (τ_0), Ratio of Correlation Times (τ_c/τ_0), Tumbling Ratios (σ) for Internal Phenylene Ring Rotation, Gierer–Wirtz Empirical Factor (f_{GW}), and Radius of Solute (r_0)

	$\tau_0 \times 10^{11}$ (s)[a]	f_{GW}[b]	r_0 (Å)[b]	τ_c/τ_0	$\sigma(D_1/D_2)$
BP5	1.8	0.30	4.8	1.06	1.0
BP6	3.9	0.39	6.8	0.57	3.5
BP6M	4.7	0.35	6.2	0.57	3.5
tBBP6	4.9	0.40	7.2	0.40[c]	6.5
				0.77[d]	1.9
tBBP6M	8.5	0.40	7.3	0.38[c]	7.0
				0.76[d]	1.9
TPBC	8.8[e]	0.40	7.4	0.31[g]	9.6
	9.9[h]	0.41	7.6	0.27[h]	12
PTB	7.5[e]	0.39	7.0	0.40[g]	6.5
	9.0[f]	0.40	7.4	0.34[h]	8.3

[a] Averaged over all protonated alicyclic carbons from T_1 data of Table 1. [b] Calculated iteratively from eq 5. [c] Ratio for the equatorial aromatic protonated carbons to cycloalkyl protonated carbons. [d] Ratio for the axial aromatic protonated carbons to cycloalkyl protonated carbons. [e] Estimated from T_1 of C_1 in Table 2. [f] Estimated from T_1 of C_7 in Table 2. [g] Ratio for T_1 of C_1 to the average T_1 of C_2 and C_3. [h] Ratio for T_1 of C_7 to the average T_1 of C_2 and C_3.

ratio of the viscosities of acetone and chloroform is 0.58. The ratio of r_0's of tBBP6 to tBBP6M was 0.58, consistent with the solvent viscosities. However, that for BP6 to BP6M was 0.83. This indicates that this estimate of the size of BP6M is too small.

The radius of the fully extended planar structure of the conjugated esters based on the crystal structure of phenyl benzoate[32] was estimated as 9.9 Å, including the van der Waals radius of hydrogen. The minimum surface area structure is globular with all three pendant groups on the same face of the central ring. Its radius is estimated to be ~5 Å. The experimental value is in fact a statistical average over all possible molecular conformations. With a single value for the correlation time, no conclusive distinction can be made. The conclusions based on the isotropic model must be treated with caution. However, as shown below, the consistent set of parameters derived from an effectively spherical model indicates that it is a reasonable approximation.

The crystal structure of phenyl benzoate[32] showed that the two phenyl rings are transoid to each other along the ester C–O bond. The dihedral angle between the planes of the phenyl ring and ester group (–COO) in the benzoate group was 9.8°. The ester phenyl ring was twisted 65.1° with respect to the –COO plane. A statistical analysis[33,34] of the X-ray diffraction data of a related series of compounds provides insight about the conformational behavior of mobile systems. The structures of phenyl carboxylates based on the Cambridge database of crystallographic data show that the phenyl group is transoid along the ester C–O single bond. This analysis also shows that the aromatic rings in RCOO–Ar esters mostly have a dihedral angle between 60° and 90°. The aromatic rings in Ar–COOR′ esters tend to orient close to the plane of ester group. The partial double-bond character of the C–O bond in the ester group is responsible for the planarity.

Phenyl acetates and phenyl formates in solution also have a transoid conformation and ~65° rotation of the phenyl ring relative to the molecular plane.

Similar low-energy conformations can be reasonably assumed for the esters in this study. The two aromatic rings will be transoid across the ester C_5–O bond. The benzoate group is close to the same plane, and the other phenyl ring will be twisted approximately 65° relative to the plane of the benzoate group. The three phenyl rings of TPBC or three benzoate rings of PTB need not be on the same side of the central aromatic ring. Comparison of these radii from model structures with r_0's obtained from the correlation times, 7.5 Å for TPBC and 7.2 Å for PTB, suggests that the conjugated esters are more globular than planar in solution. The radii of PTB and TPBC are the same with experimental error, but a slightly smaller radius is found consistently for PTB at all positions. This might suggest a more globular shape for PTB because of the bulkier benzoate groups and because the point of flexibility is closer to the central ring in PTB than in TPBC.

Internal Phenyl Rotation. Fast internal motion slows relaxation for all methyl groups and "free" aromatic rings of the molecules studied. The additional internal rotation along the C_2 axis results in longer relaxation times for the ortho and meta carbons. The shorter correlation times for these protonated phenylene ring carbons given in Tables 1 and 2 result from internal rotation superimposed on overall tumbling. From the ratio of τ_c/τ_0, the tumbling ratio, σ may be estimated from eq 11. As shown in Table 5, the estimated tumbling ratio for this set of bisphenols and methyl ethers is the same within experimental error. The solvent effect on the anisotropy of the tumbling rate seems to be comparable for the bisphenol in acetone solution and its corresponding methyl ether in chloroform solution.

There are three notable exceptions, the phenyl rings in BP5 and the axial phenylene rings in tBBP6 and tBBP6M. In BP5, the correlation time for alicyclic motion is comparable to the phenyl rotation time, and so there is no detectable differential relaxation. It is not certain whether the observed correlation time and hence effective τ_0 value are for internal libration or for overall tumbling. The two time scales are of the same order of magnitude. The σ value of the axial phenylene ring in tBBP6 and tBBP6M indicates that internal rotation in the axial position is restricted. If the molecule is spherical and the overall tumbling motion alone is responsible for the T_1 relaxation of the axial phenylene ring and the *tert*-butylcyclohexyl ring, the σ value should be 1 instead of 1.9. Some additional wobbling motion for the axial ring may affect this T_1 relaxation. The σ value of the axial phenylene ring (1.9) may represent the limit of the isotropic model used in this study and/or the maximum error range. The tumbling ratio of 7 for the equatorial phenylene ring indicates flexible internal rotation along its C_2 axis.

The σ value estimated fro BP6 and BP6M was half of the value of the equatorial phenylene ring in tBBP6 and tBBP6M. This corresponds to the average of the anisotropic tumbling ratio of axial and equatorial phenylene rings. In the limit of slow two-site exchange by ring flipping the observed relaxation rate, $1/T_{1,\mathrm{obs}}$ of BP6 and BP6M is given by the fractional sum of the axial and equatorial contributions

$$\frac{1}{T_{1,\mathrm{obs}}} = \frac{f}{T_{1,\mathrm{A}}} + \frac{1-f}{T_{1,\mathrm{E}}} = \frac{1}{2}\left(\frac{1}{T_{1,\mathrm{A}}} + \frac{1}{T_{1,\mathrm{E}}}\right) \qquad (13)$$

where f is the fractional probability of the axial contribution, which is $^1/_2$ for this system. In TPBC and PTB there is an interesting small but consistent variation in relaxation times at the four magnetic field strengths studied. All the data are internally consistent with the assumption that the benzoate group acts essentially as an effectively planar single unit. C_1 and C_7 relax at essentially the same rate, with C_7 relaxing slightly more efficiently. The C_1/C_7 differential is a little larger in PTB than TPBC. This indicates that the remote C_1 para carbon and the central C_7 carbon are relaxed by overall isotropic tumbling but that there is a little more internal motion for the phenolic-linked PTB relative to the benzoate-linked TPBC. For the internally mobile ortho and meta carbons C_2 and C_3, the C_2 rotation of the benzoate group is rapid and approximately 10% slower than that of the phenol group. This comparison for C_1 and C_2 indicates that the benzoate group maintains its transoid geometry over the rotation period.

The relaxation behavior of the quaternary carbons is particularly instructive. As shown in Figure 4, their relaxation is linearly dependent on the square of the magnetic field and dominated by CSA, particularly at high field. The slopes are given by $\Delta\sigma^2\tau_c$, and the greatest difference occurs for C_5 in PTB and TPBC. The value of $\Delta\sigma$ must be essentially identical for this carbon in the two compounds as the first point of difference is four bonds away. Thus, the slope difference must come from τ_c. The value of τ_c is lower in PTB than TPBC, which again implicates greater flexibility of the pendant benzoate group in PTB relative to the more rigid benzoate on the central ring in TPBC. With τ_c given the value for overall molecular tumbling for TPBC, $\Delta\sigma$ is calculated to be 148 ppm. This is in close agreement with the value of 153 ppm recently measured directly for the carboxyl of poly(hydroxy naphthoate).[35] This confirms that the benzoate group rotates as a rigid unit on the time scale of nanoseconds.

At 4.7 T, C_4 and C_6 relaxation is governed by equivalent dipole–dipole interactions with their ortho protons. C_4 in the pendant ring relaxes more slowly than C_6 in the central ring because it is moving more rapidly. In striking contrast, this differential relaxation is all but lost at 14.09 T where relaxation is dominated by chemical shift anisotropy. Rotation of a phenyl group about its C_2 axis provides an oscillating magnetic field, $\Delta\sigma$, as the shielding changes from σ_{33} when the ring is perpendicular to the field to σ_{11} when it is parallel. For the oxygenated ipso carbon $\Delta\sigma$ is 120 ppm from 1,3,5-trimethoxybenzene as a model[36] and is 144 ppm for the carbon bearing ipso carbon in poly(ethylene terephthalate).[37] From these model systems the shielding anisotropy for C_4 and C_6 in both esters generates an effective field of about 20 kHz at 14 T, which approaches that of a directly attached proton for DD relaxation. As an aside, the different dependence on differential rotation of DD with $\Theta = 60°$ and CSA with $\Theta = 90°$ (eqs 11 and 12) is less than 5% until the ratio of axial diffusion coefficients exceeds a factor of 10, which is not the case here. The angular dependence of the dipole–dipole relaxation follows $(1-3\cos^2\theta)$. The angular dependence of the CSA is more convoluted[38] but is more sharply peaked at values close to σ_{33}.

There are two key observations about the C_4 and C_6 relaxation in both PTB and TPBC: first, that the slopes in Figure 4 are the same within 20% whereas DD relaxation at 4.7 T showed a factor of 2 difference in their motion; second, that the value of τ_c required to match $\Delta\sigma$ with the experimental values above is that for overall tumbling. This dichotomy between DD and CSA relaxation can be resolved if one assumes that the rapid phenyl motion about its C_2 axis inhibiting DD relaxation is low-amplitude libration rather than isotropic rotational diffusion or the 180° flip required for the full effect of CSA relaxation to be experienced.

A model for calculating the different average spectral density functions for DD and CSA mechanisms for an aromatic ring was presented by Stark et al.[38] and by Tekeley[39] in his treatment of motional effects of DD relaxation in polycarbonates. The idea that small-amplitude motion is superimposed on full phenyl flips is not new. There is substantial evidence for combined motions in crystals[10] and in glassy polycarbonates.[40] This appears to be the first experimental observation of simultaneous libration and flipping for a small molecule in solution. The experimental barriers are in general agreement with the theoretical barriers for phenyl benzoate reported by Bicerano and Clark,[41] including a flat potential around the equilibrium position for the phenolic ring. Thus, these benzoate esters show that motion about the phenolic bond, C_4–O in TPBC and C_6–O in PTB, is more rapid than overall tumbling although the barrier to full rotation is at least 3 kcal/mol. On the other hand, the benzoate, bond C_5–C_6 in TPBC and C_4–C_5 in PTB, is rigid on the nanosecond time scale of overall tumbling.

Conclusions

It has been shown that phenylene motion in cycloalkylidene bisphenols and methyl ethers is generally faster than overall molecular tumbling in solution. Thus, the barrier to rotation must be less than 3 kcal/mol. By changing the cycloalkylidene ring, it is possible to modify the phenylene dynamics in parallel with the cycloalkyl ring dynamics. Thus, the order of fast phenylene motion has been found to be BP5 > BP6 eq ~ tBBP6 eq > BP6 ax ~ tBBP6 ax. The *tert*-butyl group anchors the cyclohexane ring, which in turn inhibits the motion of the axial phenylene group. The equatorial phenylene group is unaffected. The same differential motion is present in the simple cyclohexyl system, and the average value is measured. Cyclohexane ring inversion for the cyclohexylidene bisphenol is almost unaffected by the phenyl substituents. The same differential phenylene motion is found in the polycarbonates derived from these monomers in both solution and solid state.[11]

For the benzoate esters, PTB and TPBC, the phenolic C–O–C–C linkage was found to be the most flexible segment of the molecule with reorientation times which are faster than overall molecular tumbling. The dipole–dipole and chemical shift anisotropy relaxation processes for carbon in phenylene groups rotating about their C_2 axes were found to have different average diffusional correlation times. It was concluded that small-angle diffusional motion of the phenyl groups was occurring faster than overall tumbling but that full π flips were slower.

Experimental Section

Preparation of Materials. Phenyl 1,3,5-tribenzoate (PTB) was prepared by the published procedure.[42,43] ^{1}H NMR 8.20 (d, 2 H); 7.66 (t, 1 H); 7.53 (t, 2 H); and 7.18 (s, 1 H). Triphenyl 1,3,5-benzenetricarboxylate (TPBC) was prepared by reacting sodium phenoxide with 1,3,5-benzenetricarbonyl chloride (Aldrich). Sodium phenoxide (12 g, 0.1 mol) was dissolved in diglyme (80 mL) at 35 °C. To this mixture was added 1,3,5-benzenetricarbonyl chloride (8.8 g, 0.03 mol) dissolved in diglyme (6 mL). A white solid immediately formed upon addition. The reaction was maintained at 35 °C for 24 h, poured into water (500 mL), and extracted with ethyl ether. The ethereal layer was washed several times with 10% aqueous NaOH, dried, and evaporated to give cream crystals. Recrystallization from toluene yielded TPBC (3.4 g).

Synthesis of 1,1-Bis(4-hydroxyphenyl)cycloalkanes. The following general procedure[44] was used for the synthesis of the cycloalkylidene bisphenols. Phenol (22 g, 0.23 mol) was placed in a 500-mL round bottom flask and melted. The cycloalkanone (0.06 mol), 1-octanethiol (1.5 mL, 0.01 mol), and calcium chloride (2.0 g, 0.018 mol) were then added. HCl gas, produced by adding sulfuric acid to sodium chloride, was bubbled through the solution. After an hour, the solution had turned to a dark red solid. The reaction was run for an additional 4 h. The solid was recrystallized from 60/40 methanol/water to give a white solid. In some cases it was necessary to remove excess phenol by steam distillation prior to recrystallization. The starting cycloalkanones were purchased from Aldrich. The carbon NMR shifts were given in Table 1. Specific yields and characterization are as follows.

1,1-Bis(4-hydroxyphenyl)cyclohexane,[44] *BP6, and 1,1-bis(4-methoxyphenyl)cyclohexane,*[45] *BP6M,* were prepared by literature methods. *1,1-Bis(4-hydroxyphenyl)cyclopentane, BP5*: 15% yield; ^{1}H NMR (acetone-d_6) 7.12, 6.72, AA′BB′; 2.21, m; 1.64, m.

1,1-Bis(4-hydroxyphenyl)-4-tert-butylcyclohexane, tBBP6: 80% yield; ^{1}H NMR 8.13, s, OH; 8.02 s, OH; 7.20, 6.78, AA′BB′ aromatic; 6.99, 6.61, AA′BB′ aromatic; 2.67, bd d, H_{2e}; 1.82 bd t, H_{2a}; 1.68, m, H_3; 1.21, bd t, H_4; 1.17, m, CH_3; 0.74, s, C_4H_9.

1,1-Bis(4-methoxyphenyl)-4-tert-butylcyclohexane, tBBP6M, was prepared by the same procedure at BP6M. tBBP6 (2.0 g, 6.5 mmol), MeI (2.6 mL, 17.8 mmol), potassium carbonate (4.0 g, 4.0 mmol), and acetonitrile (80 mL) were placed in a 250-mL round-bottomed flask and refluxed for 20 h. The solvent was evaporated to give a yellow oil and white solid. Both were dissolved in acetonitrile and recrystallized to give tBBP6M (1.9 g, 87%, mp 77 °C). ^{1}H NMR (CD_3COCD_3) 7.25, 6.80, AA′BB′ aromatic; 7.05, 6.70, AA′BB′ aromatic; 3.70, s, OMe; 3.65, s, OMe; 2.65, bd d, H_{2e}; 1.82 bd t, H_{2a}; 1.64, m, H_3; 1.16, m, CH_3; 0.73, s, C_4H_9.

NMR Spectra. Samples were approximately 5 wt % solutions in CD_3COCD_3 for bisphenols and in $CDCl_3$ for the other samples in 5-mm NMR tubes. For the T_1 measurements of PTB and TPBC, the solutions were degassed by the freeze–pump–thaw method and sealed.

^{13}C spectra were obtained on a Varian Gemini-200 operating at 50.3 MHz, a GE QE-300 operating at 75.6 MHz, a GE OMEGA-400 operating at 100.6 MHz, and a Varian VXR-500 and a VXR-600 operating at 125.7 and 150.9 MHz, respectively. All spectra except for the NOE data were collected with continuous broad-band proton decoupling. A typical data acquisition time was 1 s and data size, 32K. The spectral window was optimized to just contain all the resonance frequencies including solvent except on the Gemini-200. A fixed spectral window (300 ppm) was used for Gemini-200 because of its fixed filter bandwidth. A 1-Hz exponential weighting of the FID was used.

Spin–lattice relaxation times for all carbons were determined simultaneously by the inversion-recovery pulse sequence (PD–180°–τ–90°). The magnetization recovery time, PD, was set greater than 5 times of the longest T_1 to be measured. The pulse delay time, τ, was varied from $T_1/4$ for the shortest T_1 to $4T_1$ for the longest T_1. Usually, 8–11 different τ values were used depending on the range of T_1 to be measured. Composite 180° pulses were used on the Varian spectrometers.

Data were analyzed by the nonlinear least-squares method provided by the software in each spectrometer. The single-exponential decay function for T_1 relaxation time was modified in the GE OMEGA-400 software to correct for incomplete inversion by the 180° pulse.

$$y = A\{1 - (W + 1)\exp(-\tau/T_1)\} \tag{14}$$

where y is the observed signal intensity at τ, A is the amplitude at $\tau = \infty$, and $W = -(A \text{ at } \tau = 0)/(A \text{ at } \tau = \infty)$ which is the correction factor for incomplete inversion. The observed signal intensity for each carbon was well fitted with eq 14. The error range in T_1 values was less than 5%. The estimated A values were 1.00 ± 0.01 with a worst case error of 0.0015. The W values depended on frequency offset from the transmitter. For aromatic carbons, W was ≥ 0.85. For the aliphatic carbons, W ranged from 0.25 to 0.75.

Acknowledgment. The generous support of the BASF Corporation through a Purdue University Industrial Associates Grant is gratefully acknowledged. Y.L. received support from a NASA Award NCC-3-128. We thank the undergraduate research participants Luke Alvey, Eugene Kogut, Wesley Romans, and Chris Wahl for sample preparation. Drs. Dean Carlson, Brett Cowans, and Perry Pellechia provided essential NMR services. Discussions with Prof. J. Caruthers, Chemical Engineering, Purdue University, initiated our interest in this project.

References and Notes

(1) Freitag, D.; Fengler, G.; Morbitzer, L. *Angew. Chem., Int. Ed. Engl.* **1991**, *30*, 1598.

(2) McHattie, J. S.; Koros, W. J.; Paul, D. R. *J. Polym. Sci.: Part B: Polym. Phys.* **1991**, *29*, 731.

(3) Sundarajan, P. R. *Macromolecules* **1990**, *23*, 2600.

(4) (a) Roy, A. K.; Jones, A. A.; Inglefield, P. T. *Macromolecules* **1986**, *19*, 1356. (b) Ratto, J. A.; Inglefield, P. T.; Rutowski, R. A.; Li, K. L.; Jones, A. A.; Roy, A. K. *J. Polym. Sci., Part B: Polym. Phys.* **1987**, *25*, 1419.

(5) (a) Jho, J. Y.; Yee, A. F. *Macromolecules* **1991**, *24*, 1905. (b) Xiao, C.; Yee, A. F. *Macromolecules* **1992**, *25*, 6800.

(6) (a) Schaefer, J.; Stejskal, E. O.; Perchak, D.; Skolnick, J.; Yaris, R. *Macromolecules* **1985**, *18*, 368. (b) Poliks, M. D.; Gullion, T.; Schaefer, J. *Macromolecules* **1990**, *23*, 2678.

(7) Garroway, A. N.; Ritchey, W. M.; Moniz, W. B. *Macromolecules* **1982**, *15*, 1051.

(8) (a) Fischer, E. W.; Hellmann, G. P.; Spiess, H. W.; Horth, F. J.; Ecarius, U.; Wehrle, M. *Makromol. Chem. Suppl.* **1985**, *12*, 189. (b) Schaefer, D.; Hansen, M.; Blumich, B.; Spiess, H. W. *J. Non-Cryst. Solids* **1991**, *131–133*, 777.

(9) Hutnik, M.; Argon, A. S.; Suter, U. W. *Macromolecules* **1991**, *24*, 5970.

(10) Henrichs, P. M.; Luss, H. R.; Scaringe, R. P. *Macromolecules* **1989**, *22*, 2731.

(11) Lee, Y.-H. Ph.D. Thesis, Purdue University, 1993.

(12) Lyerla, J. R., Jr.; Levy, G. C. In *Topics in Carbon-13 NMR Spectroscopy*; Levy, G. C., Ed.; Wiley: New York, 1974; Vol. 1, p 79.

(13) Boere, R. T.; Kidd, R. G. *Annu. Rev. NMR* **1982**, 319.

(14) (a) Heatley, F. *Prog. NMR Spectrosc.* **1979**, *13*, 47. (b) Heatley, F. *Annu. Rep. NMR Spectrosc.* **1986**, *17*, 179.

(15) Liu, F.; Horton, W. J.; Mayne, C. L.; Xiang, T.; Grant, D. M. *J. Am. Chem. Soc.* **1992**, *114*, 5281.

(16) Gierer, A.; Wirtz, K. *Z. Naturforsch.* **1953**, *A8*, 532.

(17) Farrar, T. C.; Decatur, J. D. *J. Phys. Chem.* **1990**, *94*, 7395.

(18) Levy, G. C.; Cargioli, J. D.; Anet, F. A. L. *J. Am. Chem. Soc.* **1973**, *95*, 1527.

(19) Woessner, D. E. *J. Chem. Phys.* **1962**, *37*, 647.

(20) Veeman, W. S. In *Progress in NMR Spectroscopy*; Emsley, J. W., Feeney, J., Sutcliffe, L. H., Eds.; Pergamon: Oxford, 1984; Vol. 16, p 193.

(21) Squillacote, M. E.; Neth, J. M. *J. Am. Chem. Soc.* **1987**, *109*, 198.

(22) Corio, P. L. *Structure of High Resolution NMR Spectra*; Academic Press: New York, 1961; Chapter 7.

(23) Simulations done using the software RACCOON written by Paul F. Schatz of the University of Wisconsin/Madison. The simulations were performed by trial and error.

(24) Jameson, C. J.; Osten, H. J. In *Annual Reports on NMR Spectroscopy*; Webb, G. A., Ed.; Academic Press: New York, 1986; Vol. 17, p 1.

(25) Chertkov, V. A.; Sergeyev, N. M. *J. Magn. Reson.* **1983**, *52*, 400.

(26) Sandstrom, J. *Dynamic Nuclear Magnetic Resonance Spectroscopy*; Academic Press: London, 1982; Chapter 2.

(27) (a) Dalling, D. K.; Grant, D. M.; Johnson, L. F. *J. Am. Chem. Soc.* **1971**, *93*, 3678. (b) Friebolin, H.; Schmid, H. G.; Kabuss, S.; Faisst, W. *Org. Magn. Reson.* **1969**, *1*, 147. (c) Murray, R. W.; Kaplan, M. L. *Tetrahedron* **1967**, *23*, 1574. (d) Lambert, J. B.; Gosnell, J. L.; Bailey, D. S.; Greifenstein, L. G. *J. Chem. Soc., Chem. Commun.* **1970**, 1004. (e) Kolsaker, P.; Storesund, H. J.; Schaug, J.; Larsen, G. W. *Acta Chem. Scand.* **1973**, *27*, 1460. (f) Jonas, J.; Allerhand, A.; Gutowsky, H. S. *J. Am. Chem. Soc.* **1965**, *42*, 3396. (g) Spassov, S. L.; Griffith, D. L.; Glazer, E. S.; Nagarajan, K.; Roberts, J. D. *J. Am. Chem. Soc.* **1967**, *89*, 88.

(28) *CRC Handbook of Chemistry and Physics*; CRC: Boca Raton, FL, 1985; Vol. 66, p F38.

(29) Edward, J. T. *J. Chem. Educ.* **1970**, *47*, 261.

(30) Bondi, A. *J. Phys. Chem.* **1964**, *68*, 441.

(31) Goldberg, I.; Stein, Z.; Tanaka, K.; Toda, F. *J. Inclus. Phenom.* **1988**, *6*, 15.

(32) (a) Adams, J. M.; Morsi, S. E. *Acta Crystallogr.* **1976**, *B32*, 1345. (b) The C(1)–C(6) ring and the C(8)–C(13) ring were switched on p 1346 of that paper. The torsion angle of C7–O1–C6–C1 was 67.2°, 67.1° for T(C1–C6–O1–O2), 170.0° for T(O1–C7–C8–C13), and –9.8° for T(O2–C7–C8–C13) based on the crystal data and fractional atomic coordinates of that paper.

(33) Schweizer, W.; Dunitz, J. D. *Helv. Chim. Acta* **1982**, *65*, 1547.

(34) Bredikhin, A. A.; Frolova, L. V.; Vereshchagin, A. N. *Bull. Acad. Sci. USSR, Div. Chim. Sci.* **1989**, *38*, 1422.

(35) Fyfe, C. A.; Fahie, B. J.; Lyerla, J. R.; Economy, J.; Niessner, N.; Muhlbach, A.; Facey, G. A. *Macromolecules* **1992**, *25*, 1623.

(36) (a) Sethi, N. K.; Grant, D. M.; Pugmire, R. J. *J. Magn. Reson.* **1987**, *71*, 476. (b) Carter, C. M.; Facelli, J. C.; Alderman, D. W.; Grant, D. M. *J. Chem. Soc., Faraday Trans. 1* **1988**, *84*, 3673.

(37) Murphy, P. D.; Taki, T.; Gerstein, B. C.; Henrichs, P. M.; Massa, D. J. *J. Magn. Reson.* **1982**, *49*, 99.

(38) Stark, R. E.; Vold, R. L.; Vold, R. R. *Chem. Phys.* **1977**, *20*, 337.

(39) Tekely, P. *Macromolecules* **1986**, *19*, 2544.

(40) For a summary of references see: Roy, A. K.; Inglefield, P. T. *Prog. NMR Spectrosc.* **1990**, *22*, 569.

(41) Bicerano, J.; Clark, H. A. *Macromolecules* **1988**, *21*, 585.

(42) Bredereck, H.; Heckh, H. *Chem. Ber.* **1958**, *91*, 1314.

(43) We thank the following undergraduate research participants for syntheses: Mr. A. R. Hopkins for PTB; Mr. W. L. Romans for TPBC; Mr. L. Alvey for BP5 and BP6; Mr. E. Kogut and Mr. C. Wahl for BP6M, tBBP6, and tBBP6M.

(44) Jho, H. Y.; Yee, A. F. *Macromolecules* **1991**, *24*, 1590.

(45) Meier, G.; Gerharz, B.; Boese, D.; Fischer, E. W. *J. Chem. Phys.* **1991**, *94*, 3050.